Antiferromagnetic structure of KV_2Se_2O: A neutron diffraction study

Yili Sun,[1,2,*] Yu Huang,[1,2,*] Jingwen Cheng,[1,2] Shanshan Zhang,[1,2] Zezhong Li,[1,2] Huiqian Luo,[1] Xiaobai Ma,[3,4] Wenyun Yang,[5] Jinbo Yang,[5] Dongfeng Chen,[3,4] Kai Sun,[3,4] Matthias Gutmann,[6] Silvia C. Capelli,[6] Feiran Shen,[7,8] Jiazheng Hao,[7,8] Lunhua He,[1,7,8,†] Genfu Chen,[1,2,‡] and Shiliang Li[1,2,§]

[1]*Beijing National Laboratory for Condensed Matter Physics, Institute of Physics, Chinese Academy of Sciences, Beijing 100190, China*

[2]*University of Chinese Academy of Sciences, Beijing 100049, China*

[3]*Neutron Scattering Laboratory, Department of Nuclear Physics, China Institute of Atomic Energy, Beijing 102413, People's Republic of China*

[4]*Key Laboratory of Neutron Scattering Technology and Application, China National Nuclear Corporation, Beijing 100822, China*

[5]*State Key Laboratory for Mesoscopic Physics, School of Physics, Peking University, Beijing 100871, People's Republic of China*

[6]*ISIS Neutron and Muon Source, Rutherford Appleton Laboratory, Chilton, Didcot OX11 0QX, United Kingdom*

[7]*Spallation Neutron Source Science Center, Dongguan 523803, China*

[8]*Institute of High Energy Physics, Chinese Academy of Sciences, Beijing 100049, China*

(Received 17 August 2025; revised 28 September 2025; accepted 15 October 2025; published 12 November 2025)

Altermagnetism has been proposed as a distinct class of antiferromagnets exhibiting momentum-dependent spin splitting band structures without requiring spin-orbit coupling. Recently, KV_2Se_2O has been identified as a metallic room-temperature altermagnet with d-wave spin-momentum locking. Here, we investigate the magnetic structure of KV_2Se_2O in both polycrystalline and single-crystal samples using neutron diffraction techniques. The system exhibits G-type antiferromagnetic structure with a Néel temperature $T_N \approx 400$ K. Notably, substantial broadening of magnetic peaks was observed along L at low temperatures in single crystals, consistent with the coexistence of G-type AFM order and a c-axis spin density wave. These results demonstrate that bulk KV_2Se_2O cannot host altermagnetism.

DOI: 10.1103/27n8-5q4l

I. INTRODUCTION

Altermagnetism has recently attracted significant interest due to its potential applications in spintronics and quantum information [1–6]. In altermagnets, while exhibiting antiferromagnetic (AFM) order with vanishing net magnetization, they manifest spin-dependent phenomena previously traditionally exclusive to ferromagnets through nonrelativistic spin band splitting. This behavior originates from either strong electronic correlations [7,8] or, more straightforwardly and generally, from spin-group symmetry [1,2]. In d-wave altermagnets, spin polarization undergoes sign reversal around the Fermi surface in a manner analogous to the sign change of the Cooper-pair wave function in d-wave superconductors. Several d-wave altermagnets have been experimentally confirmed, including Mn_5Si_3 [9–11], MnTe [12–14], and $MnTe_2$ [15]. However, these compounds are either semiconducting or host AFM orders below room temperature, significantly limiting their spintronics applications. Despite theoretical and experimental studies suggesting rutile RuO_2 as a room-temperature metallic d-wave altermagnet, contradictory results have been reported [16–23]. Consequently, identifying an unambiguous room-temperature metallic d-wave altermagnet remains imperative.

Recently, KV_2Se_2O was identified as a metallic room-temperature d-wave altermagnet [24]. The AV_2Q_2O family (A = K, Cs, Rb; Q = S, Se, Te) crystallizes in a tetragonal structure with alternating edge-sharing $[V_2OQ_2]^-$ layers and A^+ cations sheets stacked along the c axis. Interestingly, the V_2O planes adopt an anti-CuO_2 structure—analogous to, but inverse of, the CuO_2 planes characteristic of cuprate high-temperature superconductors. While monolayer V_2Se_2O has been theoretically predicted to exhibit interesting phenomena [25], bulk compounds in this family exhibit different properties. For instance, CsV_2S_2O is a paramagnetic bad metal [26], while CsV_2Se_2O is a semiconductor exhibiting a density-wave(DW)-like transition at 168 K [27]. KV_2Se_2O displays metallic conductivity accompanied by a DW-like transition at 105 K [28], whose origin remains debated. Proposed mechanisms include a Lifshitz transition with Fermi surface reconstruction, possibly driven by spin-density-wave (SDW) formation [29], and an SDW-driven spin canting that reduces magnetic symmetry and reconstructs the Fermi surface [30]. In contrast, Ref. [31] observed neither long-range nor short-range ordered structural phase transition but reported changes in the vanadium electronic configuration, suggesting local electronic effect.

High-temperature studies on KV_2Se_2O reveal compelling evidence for d-wave altermagnetism [24]. Nuclear magnetic resonance (NMR) measurements confirm a spin-density-wave (SDW) transition at 105 K, and further reveal a preexisting C-type AFM order above this temperature, characterized by in-plane antiferromagnetic alignment and

*These authors contributed equally to this work.
†Contact author: lhhe@iphy.ac.cn
‡Contact author: gfchen@iphy.ac.cn
§Contact author: slli@iphy.ac.cn

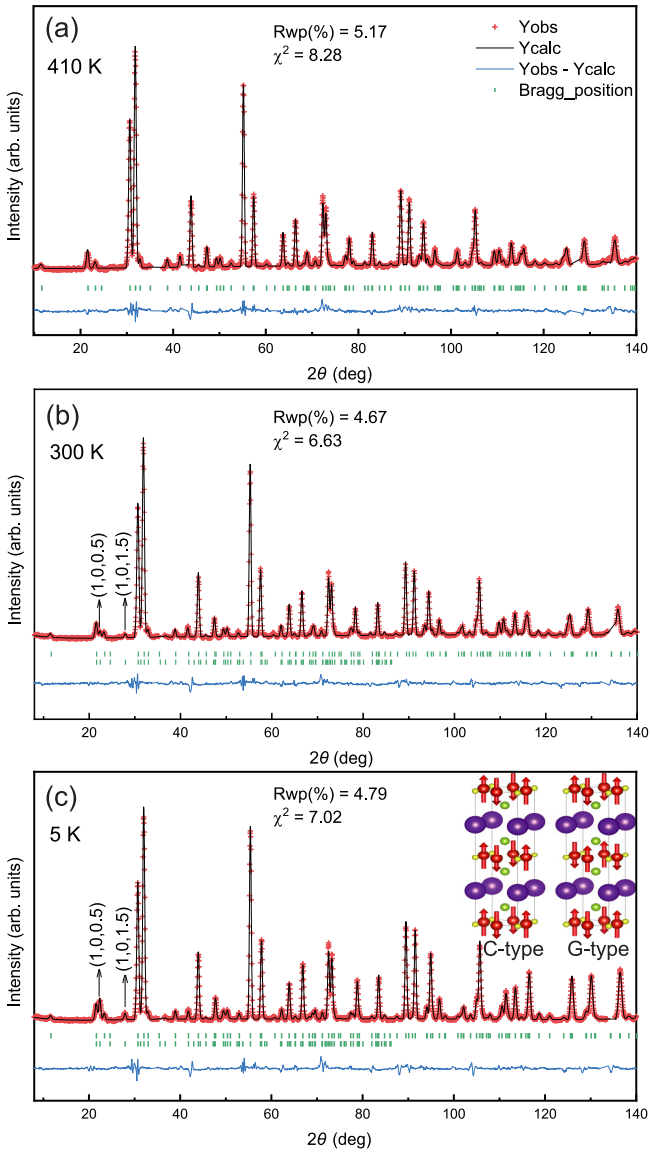

FIG. 1. Neutron diffraction results of polycrystalline KV_2Se_2O at (a) $T = 410$, (b) 300, and (c) 5 K. The observed patterns, the calculated patterns, and the difference between them are shown by red dots, black lines, and blue lines, respectively. The first row of vertical bars represents the nuclear Bragg positions, and the second row represents magnetic Bragg peak positions. The insert in (c) shows the C-type and G-type magnetic structures, the latter of which reproduces the AFM peaks emerged at 300 and 5 K.

interplane ferromagnetic coupling of vanadium spins [inset of Fig. 1(c)], with all moments parallel to the c-axis [24]. Spin- and angle-resolved photoemission spectroscopy (SARPES) demonstrates momentum-dependent spin-splitting in the band structures that is in excellent agreement with theoretical d-wave altermagnetism predictions [24], strongly suggesting KV_2Se_2O exhibits room-temperature d-wave altermagnetic behavior. Crucially, while this C-type AFM structure is essential for altermagnetism, it remains unconfirmed by diffraction methods.

In this work, we report neutron diffraction results for both single-crystal and polycrystalline samples of KV_2Se_2O. We confirm AFM order at room temperature, which vanishes at approximately 400 K. Although moments align parallel to the c axis, the magnetic structure is G-type [inset of Fig. 1(c)], characterized by antiparallel coupling between nearest neighbors along all three crystallographic axes. At low temperatures, magnetic peaks in single crystals exhibit broadening along L (c^* direction), likely arising from the superposition of G-type AFM order and a c-axis SDW. Consequently, KV_2Se_2O is not a d-wave altermagnet in its bulk form.

II. EXPERIMENTS

Polycrystalline and single-crystal samples of KV_2Se_2O were synthesized via the solid-state reaction and self-flux methods, respectively, as reported previously [28]. Notably, these samples are from the same group that provided samples in Refs. [24,28] and have checked again for consistency by magnetization measurements [32]. Since the samples are highly sensitive to moisture, all manipulations were performed in an Ar-filled glove box. Neutron powder diffraction data were collected on the High Intensity Powder Diffractometer (PKU-HIPD) at China Advanced Research Reactor (CARR) using a constant wavelength of 1.4774 Å. The polycrystalline sample was sealed in a cylindrical vanadium sample can with a diameter of 6 mm, wall thickness of 0.2 mm, and a height of 65 mm, which was put into a closed-cycle cryostat or an oven for temperature lower or higher than 300 K, respectively. Rietveld refinements were performed using the GSAS suite [33]. FULLPROF and JANA2020 have also been used to help determining the magnetic structure [34,35]. Single-crystal diffraction measurements were conducted on the SXD instrument at ISIS Facility, Rutherford Appleton Laboratory, UK [36,37]. The instrument employs the time-of-flight Laue diffraction method with polychromatic radiation in the range of 0.3–8 Å. A single-crystal sample with a smooth, flat surface and size approximately 2 mm^2 was selected under a microscope, mounted on an Al pin, and loaded into a top-loading cryo-refrigerator. Data were acquired at 5, 300, and 400 K over six distinct crystal orientations, with approximately six-hour exposure time for per orientation. Bragg diffraction spots were indexed on the basis of the unit cell obtained in the powder neutron diffraction measurements, while integrated intensities were extracted for all datasets using the methods implemented in the SXD2001 software [38].

III. RESULTS AND DISCUSSION

Figure 1(a) displays the neutron diffraction pattern of the polycrystalline sample at 410 K. Rietveld refinement confirmed the $P4/mmm$ (No.123) structure with the refined parameters aligning with the previous report [24,32]. The background was modeled using a Chebyshev polynomial of the first kind, while peak profiles were fitted using a multiterm Simpson's rule integration approach. Unindexed minor peaks stem from V_2O_3 impurities formed during synthesis and the high-temperature sample holder.

Figures 1(b) and 1(c) show the neutron diffraction patterns at 300 and 5 K, respectively. Two new peaks emerge at $2\theta = 22.42^\circ$ and 27.94°, both of which become stronger with decreasing temperature. Crucially, these peaks are absent in x-ray diffraction measurements [32], clearly demonstrating their

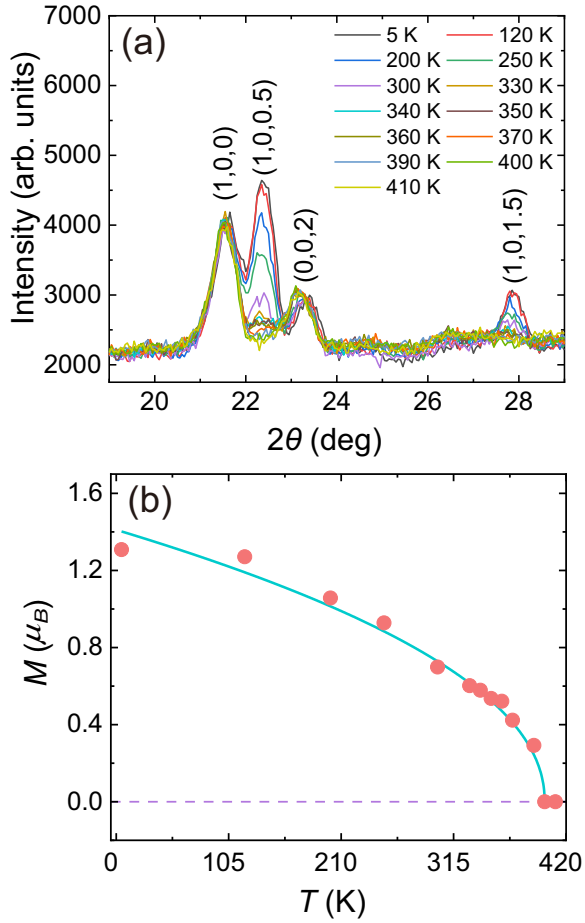

FIG. 2. (a) Neutron diffraction results of the two magnetic peaks, (1,0,0.5) and (1,0,1.5) at various temperatures for the polycrystalline KV_2Se_2O. (b) Temperature dependence of the ordered moment. The solid line is the fitted result as described in the main text.

magnetic origin. The nuclear structure remains unchanged down to 5 K [32]. All magnetic reflections can be indexed as satellites of nuclear reflections $Q_{\text{nuc}} + \mathbf{q}$, where $Q_{\text{nuc}} = Ha^* + Kb^* + Lc^*$ is a reciprocal lattice vector. Using the k_{SEARCH} program in the FULLPROF suite, we determined the propagation vector $k = (0, 0, 0.5)$. Using JANA2020, we further identified four maximal magnetic space groups compatible with the propagation vector: $P_{[c]}42/m$, $P_{[b]}21/m$, $P_{[a]}mma$, and $C_{[c]}mcm$. We tried to refine all candidate magnetic structures, such as C-type AFM order in the ab plane, or A-type AFM order with moments along c axis. However, only magnetic space group $P_{[c]}42/m$ describes correctly the diffraction pattern.

The magnetic structure of KV_2Se_2O, shown in the inset of Fig. 1(c), exhibits G-type AFM order. At 5 K, the refined ordered moment is 1.309(15) μ_B. Moments at the four V atoms within the ab-plane form a Néel-type AFM structure oriented along the c axis, consistent with theoretical predictions [24]. However, the observed AFM coupling along the c-axis contradicts the predicted C-type AFM order [24]. This magnetic ordering doubles the unit cell along c, breaking the lattice's translational symmetry along c-axis.

Figure 2(a) shows neutron diffraction patterns between $2\theta = 19^\circ$ and 29° at various temperatures, focusing on two magnetic peaks. Since magnetic peak intensity scales with the square of the ordered moment (M^2), the temperature-dependent moment magnitude was derived from the relative intensity of the (1,0,0.5) reflection normalized to its 5-K value, as shown in Fig. 2(b). We fit the temperature dependence of M below T_N to $M = M_0(1 - T/T_N)^\beta$, where M_0, T_N, and β denote the zero-temperature moment, AFM transition temperature, and critical exponent, respectively. The fitted T_N is 400.0 ± 0.7 K. The value of β is 0.48 ± 0.02, which is consistent with a Ginzburg-Landau-type transition but should be interpreted with caution [39]. This is because its value may be affected by the extensive temperature range of the fitting, as accurate determination of critical exponents requires data from the critical region near T_N. The value of M_0 is 1.41(3) μ_B corresponds to approximately half the spin-only moment for mixed-valent V^{2+}/V^{3+}. Notably, refinements used the V^{2+} and V^{3+} magnetic form factors yielded negligible differences for the above analysis.

Following the magnetic structure determination in the polycrystalline sample, we present single-crystal neutron diffraction results. Figures 3(a), 3(b), and 3(c) show symmetrized intensity colormaps in the $[H, 0, L]$ plane at 400, 300, and 5 K, respectively. The strong diffuse scattering around (0,0,0) mainly comes from the sample environment and becomes stronger at higher temperature. Consistent with the polycrystalline data, two magnetic peaks at (1,0,0.5) and (1,0,1.5) emerge at 300 K and 5 K.

Figures 4(a) and 4(b) show the cuts along the H directions at three temperatures through the (1,0,0.5) and (1,0,1.5) positions, respectively. These scans clearly demonstrates the emergence of magnetic peaks at 300 and 5 K. At the (1,0,0.5) position, a weak peak persists at 400 K, suggesting the T_N of the single crystal may exceed that of the polycrystalline sample, which needs to be studied in the future. Notably, the peaks are very sharp and their widths are beyond the instrumental resolution. As shown in Figs. 4(e) and 4(f), while both peaks show narrow L-scans at 300 K, they become two to three times broader at 5 K.

Our results establish that both polycrystalline and single-crystal samples exhibit G-type AFM order at 300 K. This structure fundamentally differs from the theoretically proposed C-type AFM structure–a prerequisite for realizing d-wave altermagnetism in KV_2Se_2O [24]. While SARPES measurements reveal highly anisotropic spin-polarized Fermi surfaces [24], we note that this technique only probes surface electronic states. Given the weak interlayer coupling between V_2Se_2O layers and near-degeneracy of C-type and G-type AFM ground states, we cannot exclude the possibility that the surface region hosts the C-type AFM order [25], potentially explaining the observed altermagnetic-like band structures in KV_2Se_2O. It should be noted that this is a hypothesis which demands future work.

Previous studies have identified a phase transition at 105 K in single-crystal KV_2Se_2O. The SDW nature of the transition is evidenced by the sharp increase of the resistivity at the transition followed by a resurgence of metallic behavior with decreasing temperature, the suppression of c-axis magnetic susceptibility, a substantial increase in Hall coefficient, and the splitting of NMR spectra below the transition [24,28]. Intriguingly, while a small energy gap opens in the SDW state,

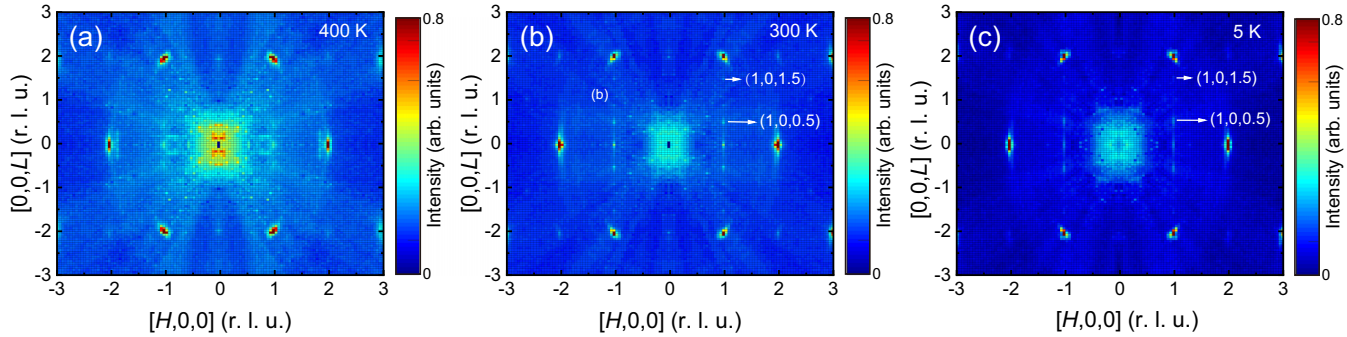

FIG. 3. [(a), (b), and (c)] Distribution of symmetrized single crystal neutron diffraction patterns in the [H, 0, L] plane at 400, 300, and 5 K, respectively. The (1,0,0.5) and (1,0,1.5) magnetic peaks are labeled in (b) and (c).

the gap feature persists well above the transition temperature without coherence peaks, indicating pseudogap behavior [24].

Intriguingly, the low-temperature magnetic susceptibility and specific heat exhibit differences between polycrystalline and single-crystal samples [28]. While the DW-like transition at 105 K is clearly revealed in single crystals, it is not observed in polycrystalline samples. This difference could potentially come from stoichiometric variations of the alkali metal, a phenomenon observed in other compounds such as NaFeAs, where superconductivity can be induced by Na deficiencies [40,41]. Although the effects of these stoichiometric variations require further investigation, we note that the room-temperature magnetic structures are identical for polycrystalline and single-crystal samples. Consistent with this, our results show that magnetic peaks in the polycrystalline sample evolve continuously with temperature, showing no sign of a low-temperature magnetic transition. In contrast, the magnetic peaks in the single-crystal sample become significantly broader along the L direction at 5 K. Previous studies have shown that the ^{51}V NMR spectra at zero field changes from a single peak above 100 K to two peaks below it, suggesting two distinct magnetic moment magnitudes [24]. Although the proposed interpretation relies on nesting within in-plane Fermi surfaces, which would double the in-plane magnetic unit cell, we find no new magnetic peaks at 5 K, thereby challenging this picture. Notably, the AFM structure is G-type rather than the proposed C-type structure [24]. Consequently, symmetry remains unchanged with alternate changes in moment magnitude along the c axis. While our single-crystal data lack sufficient quality for definitive refinement [32], the broadening of magnetic peaks along the L direction may result from the superposition of a c-axis SDW onto the G-type AFM order, which could reduce the c-axis magnetic correlation length. This proposed picture requires confirmation from future studies.

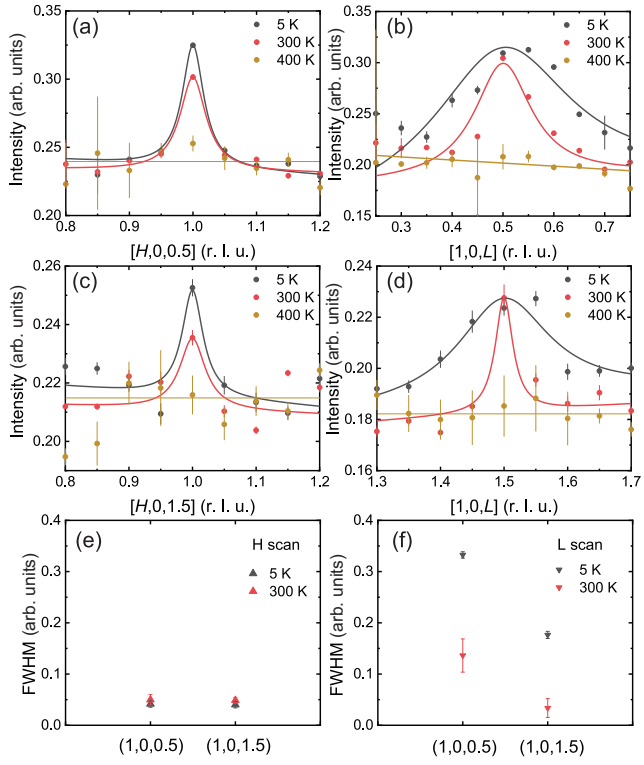

FIG. 4. [(a) and (b)] Cuts along the H and L directions through the (1,0,0.5) position, respectively. [(c) and (d)] Cuts along the H and L directions through the (1,0,1.5) position, respectively. The solid lines are fitted results using either a Gaussian function at 300 and 5 K or a linear function at 400 K. (e) and (f) FWHMs along H and L directions, respectively, at 5 and 300 K.

IV. CONCLUSIONS

In conclusion, our neutron diffraction study establishes a G-type AFM order in both polycrystalline and single-crystal KV_2Se_2O at room temperature, contradicting the proposed C-type structure essential for d-wave altermagnetism. Consequently, bulk KV_2Se_2O is not an altermagnet. At low temperatures, single crystals exhibit significant magnetic peak broadening along the L direction, likely arising from a coexisting c-axis SDW modulating the G-type order without breaking symmetry. These results strongly constrain future investigations of d-wave altermagnetism in KV_2Se_2O.

ACKNOWLEDGMENTS

S.L. acknowledges helpful discussions with Tian Qian, Quansheng Wu, Junwei Liu, and Zheng Li. This work is supported by the National Key Research and Development Program of China (Grants No. 2022YFA1403400, No. 2021YFA1400400, No. 2022YFA1403903, No. 2022YFA1403800, and No. 2023YFA1406100), and the National Natural Science Foundation of China (Grants No.

12274440, No. 12241401, No. 12274444, No. 11974392, and No. 12574165).

DATA AVAILABILITY

Some of the data that support the findings of this article are openly available [37]. Diffraction data for the polycrystalline sample are not publicly available upon publication because it is not technically feasible and/or the cost of preparing, depositing, and hosting the data would be prohibitive within the terms of this research project. The data are available from the authors upon reasonable request.

[1] L. Šmejkal, J. Sinova, and T. Jungwirth, Emerging research landscape of altermagnetism, Phys. Rev. X **12**, 040501 (2022).

[2] L. Šmejkal, J. Sinova, and T. Jungwirth, Beyond conventional ferromagnetism and antiferromagnetism: A phase with nonrelativistic spin and crystal rotation symmetry, Phys. Rev. X **12**, 031042 (2022).

[3] L. Bai, W. Feng, S. Liu, L. Šmejkal, Y. Mokrousov, and Y. Yao, Altermagnetism: Exploring new frontiers in magnetism and spintronics, Adv. Funct. Mater. **34**, 2409327 (2024).

[4] S. S. Fender, O. Gonzalez, and D. K. Bediako, Altermagnetism: A chemical perspective, J. Am. Chem. Soc. **147**, 2257 (2025).

[5] C. Song, H. Bai, Z. Zhou, L. Han, H. Reichlova, J. H. Dil, J. Liu, X. Chen, and F. Pan, Altermagnets as a new class of functional materials, Nat. Rev. Mater. **10**, 473 (2025).

[6] T. Jungwirth, R. M. Fernandes, E. Fradkin, A. H. MacDonald, J. Sinova, and L. Šmejkal, Altermagnetism: An unconventional spin-ordered phase of matter, Newton **1**, 100162 (2025).

[7] C. Wu, K. Sun, E. Fradkin, and S.-C. Zhang, Fermi liquid instabilities in the spin channel, Phys. Rev. B **75**, 115103 (2007).

[8] L. Classen, A. V. Chubukov, C. Honerkamp, and M. M. Scherer, Competing orders at higher-order van Hove points, Phys. Rev. B **102**, 125141 (2020).

[9] H. Reichlova, R. L. Seeger, R. González-Hernández, I. Kounta, R. Schlitz, D. Kriegner, P. Ritzinger, M. Lammel, M. Leiviskä, A. B. Hellenes, K. Olejník, V. Petříček, P. Doležal, L. Horak, E. Schmoranzerova, A. Badura, S. Bertaina, A. Thomas, V. Baltz, L. Michez *et al.*, Observation of a spontaneous anomalous Hall response in the Mn_5Si_3 d-wave altermagnet candidate, Nat. Commun. **15**, 4961 (2024).

[10] J. Rial, M. Leiviskä, G. Skobjin, A. Bad'ura, G. Gaudin, F. Disdier, R. Schlitz, I. Kounta, S. Beckert, D. Kriegner, A. Thomas, E. Schmoranzerová, L. Šmejkal, J. Sinova, T. c. v. Jungwirth, L. Michez, H. Reichlová, S. T. B. Goennenwein, O. Gomonay, and V. Baltz, Altermagnetic variants in thin films of Mn_5Si_3, Phys. Rev. B **110**, L220411 (2024).

[11] T. Osumi, S. Souma, T. Aoyama, K. Yamauchi, A. Honma, K. Nakayama, T. Takahashi, K. Ohgushi, and T. Sato, Observation of a giant band splitting in altermagnetic MnTe, Phys. Rev. B **109**, 115102 (2024).

[12] J. Krempaský, L. Šmejkal, S. D'souza, M. Hajlaoui, G. Springholz, K. Uhlířová, F. Alarab, P. Constantinou, V. Strocov, D. Usanov *et al.*, Altermagnetic lifting of Kramers spin degeneracy, Nature (London) **626**, 517 (2024).

[13] S. Lee, S. Lee, S. Jung, J. Jung, D. Kim, Y. Lee, B. Seok, J. Kim, B. G. Park, L. Šmejkal, C.-J. Kang, and C. Kim, Broken Kramers degeneracy in altermagnetic MnTe, Phys. Rev. Lett. **132**, 036702 (2024).

[14] O. J. Amin, A. D. Din, E. Golias, Y. Niu, A. Zakharov, S. C. Fromage, C. J. B. Fields, S. L. Heywood, R. B. Cousins, F. Maccherozzi, J. Krempaský, J. H. Dil, D. Kriegner, B. Kiraly, R. P. Campion, A. W. Rushforth, K. W. Edmonds, S. S. Dhesi, L. Šmejkal, T. Jungwirth *et al.*, Nanoscale imaging and control of altermagnetism in MnTe, Nature (London) **636**, 348 (2024).

[15] Y.-P. Zhu, X. Chen, X.-R. Liu, Y. Liu, P. Liu, H. Zha, G. Qu, C. Hong, J. Li, Z. Jiang *et al.*, Observation of plaid-like spin splitting in a noncoplanar antiferromagnet, Nature (London) **626**, 523 (2024).

[16] Z. H. Zhu, J. Strempfer, R. R. Rao, C. A. Occhialini, J. Pelliciari, Y. Choi, T. Kawaguchi, H. You, J. F. Mitchell, Y. Shao-Horn, and R. Comin, Anomalous antiferromagnetism in metallic RuO_2 determined by resonant x-ray scattering, Phys. Rev. Lett. **122**, 017202 (2019).

[17] A. Bose, N. J. Schreiber, R. Jain, D.-F. Shao, H. P. Nair, J. Sun, X. S. Zhang, D. A. Muller, E. Y. Tsymbal, D. G. Schlom, and D. C. Ralph, Tilted spin current generated by the collinear antiferromagnet ruthenium dioxide, Nat. Electron. **5**, 267 (2022).

[18] H. Bai, L. Han, X. Y. Feng, Y. J. Zhou, R. X. Su, Q. Wang, L. Y. Liao, W. X. Zhu, X. Z. Chen, F. Pan, X. L. Fan, and C. Song, Observation of spin splitting torque in a collinear antiferromagnet RuO_2, Phys. Rev. Lett. **128**, 197202 (2022).

[19] S. Karube, T. Tanaka, D. Sugawara, N. Kadoguchi, M. Kohda, and J. Nitta, Observation of spin-splitter torque in collinear antiferromagnetic RuO_2, Phys. Rev. Lett. **129**, 137201 (2022).

[20] Z. Lin, D. Chen, W. Lu, X. Liang, S. Feng, K. Yamagami, J. Osiecki, M. Leandersson, B. Thiagarajan, J. Liu *et al.*, Observation of giant spin splitting and d-wave spin texture in room temperature altermagnet RuO_2, arXiv:2402.04995.

[21] M. Hiraishi, H. Okabe, A. Koda, R. Kadono, T. Muroi, D. Hirai, and Z. Hiroi, Nonmagnetic ground state in RuO_2 revealed by muon spin rotation, Phys. Rev. Lett. **132**, 166702 (2024).

[22] J. Liu, J. Zhan, T. Li, J. Liu, S. Cheng, Y. Shi, L. Deng, M. Zhang, C. Li, J. Ding, Q. Jiang, M. Ye, Z. Liu, Z. Jiang, S. Wang, Q. Li, Y. Xie, Y. Wang, S. Qiao, J. Wen *et al.*, Absence of altermagnetic spin splitting character in rutile oxide RuO_2, Phys. Rev. Lett. **133**, 176401 (2024).

[23] L. Kiefer, F. Wirth, A. Bertin, P. Becker, L. Bohatý, K. Schmalzl, A. Stunault, J. A. Rodríguez-Velamazán, O. Fabelo, and M. Braden, Crystal structure and absence of magnetic order in single-crystalline RuO_2, J. Phys.: Condens. Matter **37**, 135801 (2025).

[24] B. Jiang, M. Hu, J. Bai, Z. Song, C. Mu, G. Qu, W. Li, W. Zhu, H. Pi, Z. Wei, Y.-J. Sun, Y. Huang, X. Zheng, Y. Peng, L. He, S. Li, J. Luo, Z. Li, G. Chen, H. Li *et al.*, A metallic room-temperature d-wave altermagnet, Nat. Phys. **21**, 754 (2025).

[25] H.-Y. Ma, M. Hu, N. Li, J. Liu, W. Yao, J.-F. Jia, and J. Liu, Multifunctional antiferromagnetic materials with giant

piezomagnetism and noncollinear spin current, Nat. Commun. **12**, 2846 (2021).

[26] M. Valldor, P. Merz, Y. Prots, and W. Schnelle, Bad-metal-layered sulfide oxide CsV_2S_2O, Eur. J. Inorg. Chem. **2016**, 23 (2016).

[27] H. Lin, J. Si, X. Zhu, K. Cai, H. Li, L. Kong, X. Yu, and H.-H. Wen, Structure and physical properties of $CsV_2Se_{2-x}O$ and V_2Se_2O, Phys. Rev. B **98**, 075132 (2018).

[28] J. Bai, B. Ruan, Q. Dong, L. Zhang, Q. Liu, J. Cheng, P. Liu, C. Li, Y. Sun, Y. Huang *et al.*, Absence of long-range order in the vanadium oxychalcogenide KV_2Se_2O with nontrivial band topology, Phys. Rev. B **110**, 165151 (2024).

[29] Y. Xu, H. Zhang, M. Feng, and F. Tian, Electronic structure, magnetic transition, and Fermi surface instability of the room-temperature altermagnet KV_2Se_2O, Phys. Rev. B **112**, 125141 (2025).

[30] X. Yan, Z. Song, J. Song, Z. Fang, H. Weng, and Q. Wu, SDW driven "magnetic breakdown" a d-wave altermagnet KV_2Se_2O, arXiv:2505.00074.

[31] H. Zhuang, J. Bai, J. Cheng, X. Li, Y. Meng, L. Wang, Q. Zhang, X. Shen, Y. Wang, G. Chen, and R. Yu, Charge transfer caused anomalies of physical properties of KV_2Se_2O, Europhys. Lett. **150**, 36003 (2025).

[32] See Supplemental Material at http://link.aps.org/supplemental/10.1103/27n8-5q4l for further refinement results of neutron powder and single-crystal diffraction data, single-crystal XRD data, and magnetization measurements.

[33] A. C. Larson and R. B. Von Dreele, General structure analysis system (GSAS), Los Alamos National Laboratory Report LAUR 86-748 (2004).

[34] J. Rodríguez-Carvajal, Recent advances in magnetic structure determination by neutron powder diffraction, Phys. B: Condens. Matter **192**, 55 (1993).

[35] V. Petříček, L. Palatinus, J. Plášil, and M. Dušek, Jana2020–A new version of the crystallographic computing system jana, Z. Kristallogr. **238**, 271 (2023).

[36] D. A. Keen, M. J. Gutmann, and C. C. Wilson, SXD–the single-crystal diffractometer at the isis spallation neutron source, J. Appl. Cryst. **39**, 714 (2006).

[37] Y. Sun, S. Zhang, M. Gutmann, D. Adroja, and H. Luo, Magnetic structure of a new kagome topological semimetal $Ni_3In_2Se_2$, STFC ISIS neutron and muon source (2025), doi:10.5286/ISIS.E.RB2510001.

[38] M. J. Gutmann, Sxd2001–A program for treating data from tof neutron single-crystal diffraction, Acta Cryst. A **61**, c164 (2005).

[39] M. F. Collins, *Magnetic Critical Scattering* (Oxford University Press, Oxford, 1989).

[40] G. F. Chen, W. Z. Hu, J. L. Luo, and N. L. Wang, Multiple phase transitions in single-crystalline $Na_{1-\delta}FeAs$, Phys. Rev. Lett. **102**, 227004 (2009).

[41] I. Todorov, D. Y. Chung, H. Claus, C. D. Malliakas, A. P. Douvalis, T. Bakas, J. He, V. P. Dravid, and M. G. Kanatzidis, Topotactic redox chemistry of nafeas in water and air and superconducting behavior with stoichiometry change, Chem. Mater. **22**, 3916 (2010).